

ATP Synthase and Neuroglobin as Factors Determining the Path of Neuronal Destruction in Cerebral Ischemia



LV Uzlova, SM Zimatkin and LI Bon*

Grodno State Medical University, 80, Gorkogo St., 230009, Grodno, Republic of Belarus, Russia

*Corresponding author: Lizaveta I Bon, Candidate of biological science, assistant professor of pathophysiology department named D.A. Maslakov, Grodno State Medical University and Grodno State Medical University, 80, Gorky St., 230009, Grodno, Belarus, Russia

ARTICLE INFO

Received: September 23, 2022

Published: October 06, 2022

ABSTRACT

Citation: LV Uzlova, SM Zimatkin and LI Bon. ATP Synthase and Neuroglobin as Factors Determining the Path of Neuronal Destruction in Cerebral Ischemia. Biomed J Sci & Tech Res 46(3)-2022. BJSTR. MS.ID.007363.

Financing

The study was carried out within the framework of the project "Assessment of the energy potential and oxygen depot of brain neurons to predict their sensitivity to ischemia" of the Belarusian Republican Foundation for Fundamental Research Nauka-M (Registration No: 20213456, 20.09.2021).

Introduction

The brain is extremely vulnerable to blood flow disorders. If it is disturbed, cerebral ischemia develops. Since the degree of damage to neurons depends on the duration of cerebral ischemia, regional characteristics of vulnerability and many other factors, the pressing issue is an integrated study of the disorders occurring in neurons and their cooperation, as well as the pressing issue is the content of markers such as ATP synthase, which reflects the energy potential of neurons of various types and parts of the brain, and oxygen-binding protein neuroglobin (Ngb), because there is no data on their relationship.

Aim of the Study

Aim of the study is to examine changes in cytoplasmic chromatophilia in populations of neurons in various parts of the

rat brain during experimental ischemia and relationships of these changes with the content and dynamics of ATP synthase and Ngb.

Methods

The permission to conduct the study was obtained on January 15, 2020, from the Biomedical Ethics Committee of the Grodno State Medical University. The study was carried out in accordance with the requirements of the Directive of the European Parliament and of the Council No:2010/63/EU of September 22, 2010, on the protection of animals used for scientific purposes.

Material from 12 white male rats weighing 230 ± 20 g was used in the study. When modeling subtotal cerebral ischemia (SCI), all rats were anesthetized by intravenous administration of 40-50 mg/kg of sodium thiopental. A 2 cm long incision was made along the midline of the ventral cervical surface, exposing the common carotid arteries. In animals of the experimental groups - 30-minute SCI and 3-hour SCI - simultaneous ligation of both common carotid arteries was carried out, while in animals of the control group arterial ligation was not performed and the incision was sutured. Animals were derived from the experiment immediately after the operation (for rats of the control group), and 30 minutes and 3 hours after the operation (for rats of the experimental groups). The brain was

quickly removed after decapitation and divided into three parts by frontal incisions. All samples were fixed in a combined fixative - zinc-ethanol-formaldehyde at +4°C for 20 hours. After dehydration, clarification, and paraffin embedding, frontal serial sections 5 µm thick were made every 500 µm using a Leica 2125 RTS microtome (Germany) and mounted on adhesive-coated glass slides.

The first section from each series was stained with 0.1% toluidine blue according to the Nissl method to reveal the chromatophilic substance of neurons and identify brain structures according to stereotaxic atlas [1]. The following groups of neurons were distinguished when assessing the chromatophilia of the cytoplasm: normochromic (moderately stained), hyperchromic (intensely stained), hyperchromic shriveled up (intensely stained with shriveled up perikarya), hypochromic (weakly stained) and shadow cells (very weakly stained, with a pale bubble-shaped nucleus). The degree of sensitivity of neurons to ischemia was determined by the degree of these changes compared with the control, as well as by the predominance of reversible (increase in the number of hyperchromic and hypochromic neurons) or irreversible changes (increase in the number of hyperchromic shriveled up neurons and shadow cells). The nature of chromatophilia was assessed in 60 areas of the brain: layers of the cortex and nuclei of the brain. Neuron cytoplasmic chromatophilia was assessed and counted in 10 fields of view at ×400 for each structure per animal, which provided sufficient data even for structures characterized by a relatively small number of neurons.

The second section from each series was stained using the Viktorov method to identify brightly stained fuchsinophilic dying neurons [2]. The third and fourth sections were stained immunohistochemically. To assess the immunoreactivity of ATP synthase, primary monoclonal mouse antibodies Anti-ATP5A antibody (Abcam, UK, ab. 14748) were used at a dilution of 1:2400 at +4 °C exposure 20 h in a humid chamber. To determine the immunoreactivity of Ngb, primary monoclonal mouse antibodies (Anti-Ngb antibody from Abcam, UK, ab. 14748) were used at a

dilution of 1:600 (chosen as optimal from a series of dilutions from 1:100 to 1:3000) at +4 °C exposure 20 h in a humid chamber. In both cases, Mouse and Rabbit Specific HRP/DAB IHC Detection Kit - Micro-polymer (UK, Abcam, ab236466) was used to detect bound primary antibodies. The immunoreactivity of ATP synthase and Ngb was studied in 25 structures of the rat brain.

Preparations were studied, microphotographed, and cytophotometrically performed using Axioskop 2 plus microscope (Zeiss, Germany), Leica DFC 320 digital video camera (Leica Microsystems GmbH, Germany), and Image Warp computer image analysis program (Bit Flow, USA). Immunoreactivity was expressed in units of optical density ×103 (arbitrary units - a.u.). The obtained quantitative continuous data were processed by the methods of descriptive and nonparametric statistics using the licensed computer program Statistica 10.0 for Windows (StatSoft, Inc., USA, serial number AXAR207F394425FA-Q). Non-parametric Mann-Whitney U-criteria, Kruskal-Wallis H-criteria and Spearman rank correlation coefficient was used (probability of an erroneous estimate should not exceed 5%).

Results

Histological disorders in neurons of different parts of the rat brain during ischemia. In animals of the control group normochromic and hyperchromic neurons predominate in all parts/structures of the brain (Table 1). After a 30-minute ischemia in most structures of the rat brain there is a decrease in the number of normochromic and an increase in the number of hyperchromic, hyperchromic shriveled up, hypochromic and shadow cells (Table 1). However, neurons resistant to 30-minute ischemia are also found in various parts of the brain (Table 1). After a 3-hour ischemia the proportion of normochromic neurons decreases and the proportion of hyperchromic, hyperchromic shriveled up, hypochromic neurons and shadow cells increases in all studied brain structures. Absolutely resistant to 3-hour SCI brain structures were not found (Table 1).

Table 1: Ratio of neuron types with different degrees of cytoplasmic chromatophilia in rat brain structures after SCI (in %; *p<0.05).

Structure, group	Type of neurons according to the degree of chromatophilia of the cytoplasm				
	normochromic	hyperchromic	hyperchromic shriveled up	hypochromic	shadow cells
Telencephalon					
Mitral cells of the olfactory bulb	control	44,5	37,5	11,1	6,9
	30 min	5,5 ↓*	21,8	39,1 ↑*	23,6 *
	3 h	9,6 ↓*	10,8	67,5 ↑*	7,2
Piriform cortex, layer II	control	35,4	34	22,3	8,3
	30 min	37,2	13,6 ↓*	22,0	21,5
	3 h	10,8 ↓*	17,9 ↓*	55,1	10,8

Hippocampus CA1, layer II	control	78,1	3,3	1,9	12,6	4,1
	30 min	8,1 ↓*	28,5 ↑*	49,6 ↑*	6,5	7,3
	3 h	0 ↓*	11,9 ↑*	72,4 ↑*	10,1	5,6
Hippocampus CA2, layer II	control	78,4	7	5,9	8	0,7
	30 min	13,2 ↓*	36 ↑*	44,6 ↑*	5,3	0,9
	3 h	14,1 ↓*	35,7 ↑*	34,3 ↑*	8,3	7,6
Hippocampus CA3, layer II	control	39	27,8	24,9	5,3	3
	30 min	7 ↓*	33,2	51,3 ↑*	3,2	5,3
	3 h	1,5 ↓*	24,4	63,7 ↑*	8,3	2,1
Dentate gyrus, layer II	control	57,9	16,8	10,6	12,4	2,3
	30 min	17,4 ↓*	32,1	34,3 ↑*	10,8	5,4
	3 h	7,8 ↓*	30,4	41,9 ↑*	11,4	8,5 ↑*
Cingulate cortex, layer II	control	86,9	0,9	1,9	8,4	1,9
	30 min	39,1	5,1	9,6 ↑*	30,8 ↑*	15,4 ↑*
	3 h	6,8 ↓*	44,8 ↑*	17,1 ↑*	13,9 ↑*	17,3 ↑*
Cingulate cortex, layer III	control	66,4	7,4	5,7	13,1	7,4
	30 min	39	14,6	13	17,9	15,5
	3 h	2,4 ↓*	35,4 ↑*	15,1 ↑*	42,8 ↑*	4,2
Cingulate cortex, layer V	control	68	13	2	10	7
	30 min	27,9 ↓*	31,4	7	19,8 ↑*	13,9
	3 h	3,9 ↓*	45,5 ↑*	19,6 ↑*	28,6 ↑*	2,4
Cingulate cortex, layer VI	control	41,2	8	10,5	22,8	17,5
	30 min	26,6 ↓*	13,9	24,1	16,5	18,9
	3 h	0 ↓*	7,4	69,6 ↑*	22	1 ↓*
Retrosplenial agranular cortex, layer II	control	56,7	43,0	0,3	0	0
	30 min	10,4 ↓*	74,9 ↑*	10,6 ↑*	4,2 ↑*	0
	3 h	0 ↓*	63,3 ↑*	21,8 ↑*	13,9 ↑*	1,0
Retrosplenial agranular cortex, layer III	control	73,6	26,4	0	0	0
	30 min	10,8 ↓*	75,3 ↑*	9,4 ↑*	3,8	0,7
	3 h	0 ↓*	48,7 ↑*	33,8 ↑*	14,5 ↑*	3
Retrosplenial agranular cortex, layer V	control	54,1	45,9	0	0	0
	30 min	10,1 ↓*	76,4 ↑*	11,5 ↑*	2	0
	3 h	0 ↓*	18,2 ↓*	60,6 ↑*	18,5 ↑*	2,7
Retrosplenial agranular cortex, layer VI	control	42,9	56	1,1	0	0
	30 min	0,3 ↓*	76,7 ↑*	13,3 ↑*	8,5 ↑*	1,2
	3 h	0 ↓*	34	43 ↑*	19,5 ↑*	3,6 ↑*
Temporal cortex, layer II	control	57,1	41,4	0,9	0,6	0
	30 min	9,1 ↓*	85,2 ↑*	4,9 ↑*	0,8	0
	3 h	25,1	7,0 ↓*	5,8 ↑*	47,4 ↑*	14,6 ↑*
Temporal cortex, layer III	control	37,4	57,3	5,3	0	0
	30 min	14,6 ↓*	74,5 ↑*	7,2	3,4	0,3
	3 h	25,6	4,3 ↓*	7,8	54,7 ↑*	7,6 ↑*
Temporal cortex, layer IV	control	29,4	61,9	8,1	0,6	0
	30 min	10,3 ↓*	73 ↑*	11,2 ↑*	4,5 ↑*	1
	3 h	32,4	3,6 ↓*	3,0	53,4 ↑*	7,6 ↑*

Temporal cortex, layer V	control	27,6	56,4	16	0	0
	30 min	12,3 ↓*	70,2 ↑*	10,5	5,5 ↑*	1,5
	3 h	15,3 ↓*	8,1 ↓*	23,6	46,8 ↑*	6,3 ↑*
Temporal cortex, layer VI	control	22,8	73,9	3	0,3	0
	30 min	17,5	66,5 ↓*	8,8 ↑*	6 ↑*	1,2
	3 h	12,4 ↓*	9,5 ↓*	23,3	51,0 ↑*	3,8 ↑*
Motor cortex, layer II	control	75,6	7	0	15,7	1,7
	30 min	19,7 ↓*	24,1 ↑*	14,6 ↑*	26,3 ↑*	15,3 ↑*
	3 h	14,9 ↓*	9	12,4 ↑*	51,1 ↑*	12,6 ↑*
Motor cortex, layer III	control	66,4	17,2	0,8	12,3	3,3
	30 min	22,6	24,9	11,9 ↑*	23,1 ↑*	17,5 ↑*
	3 h	18,8	7,2	5,9	51,2 ↑*	17,0 ↑*
Motor cortex, layer V	control	56,7	6	2,4	28,9	6
	30 min	27,3 ↓*	29,5 ↑*	6,8	28,4	8
	3 h	13 ↓*	21,6	17,8 ↑*	41,3 ↑*	6,3
Motor cortex, layer VI	control	64,8	7,2	3,2	24,8	0
	30 min	36,7 ↓*	19,4 ↑*	13,3 ↑*	25,5	5,1
	3 h	2,7 ↓*	11,1	46,8 ↑*	32,3	7,1 ↑*
Occipital cortex, layer II	control	63,1	3,9	0,4	18,6	14
	30 min	23,6 ↓*	21,8 ↑*	5,1	28,2	21,3
	3 h	0 ↓*	15,6	0,5	62,3 ↑*	21,7 ↑*
Occipital cortex, layer III	control	65,3	4,6	0,6	18,6	10,9
	30 min	24,7 ↓*	24 ↑*	4,9 ↑*	27,6	18,8 ↑*
	3 h	4,2 ↓*	4,2	0,4	64,6 ↑*	26,6 ↑*
Occipital cortex, layer IV	control	59,8	12,5	2,3	14	11,4
	30 min	10,2 ↓*	32 ↑*	7,8	35,4 ↑*	14,6
	3 h	0,5 ↓*	4,4	2	74,9 ↑*	18,2
Occipital cortex, layer V	control	54,9	23,8	1,8	16,5	3
	30 min	4,8 ↓*	42,4	30 ↑*	18	4,8
	3 h	6,3 ↓*	26,3	7	48,9 ↑*	11,5 ↑*
Occipital cortex, layer VI	control	44,7	26,8	10,6	14	3,9
	30 min	1,4 ↓*	10,6	65 ↑*	20,3	2,7
	3 h	0 ↓*	6,3	16,0	69,4 ↑*	8,3 ↑*
Diencephalon						
Medial habenula of the thalamus	control	12,3	85,3	2,4	0	0
	30 min	8,2	79,1	11,5 ↑*	1,2	0
	3 h	0,2 ↓*	1,2 ↓*	65,6 ↑*	28,6 ↑*	4,4 ↑*
Paraventricular thalamic nucleus	control	18,3	79,8	1,9	0	0
	30 min	10	48,8	41,2 ↑*	0	0
	3 h	0 ↓*	9,9 ↓*	84,7 ↑*	5,4 ↑*	0
Lateral posterior thalamic nucleus	control	27,8	66,2	5,7	0,3	0
	30 min	19,8 ↓*	28,1 ↓*	47,4 ↑*	4,4 ↑*	0,3
	3 h	1,6 ↓*	21,2 ↓*	59,5 ↑*	16,1 ↑*	1,6
Lateral hypothalamic area	control	48,9	46	5,1	0	0
	30 min	25,9	58 ↑*	12,1 ↑*	3,8 ↑*	0,2
	3 h	11,1 ↓*	23,0 ↓*	45,1 ↑*	15,9 ↑*	4,9 ↑*

Medial mammillary nucleus	control	26,9	53	8,2	6,8	5,1
	30 min	10,5	4,2 ↓*	49,7 ↑*	22,9 ↑*	12,7 ↑*
	3 h	0 ↓*	0 ↓*	12,8	58,9 ↑*	28,3 ↑*
Supramammillary nucleus	control	44,3	39	1,3	14,1	1,3
	30 min	20,5	5 ↓*	38,3 ↑*	25,6	10,6 ↑*
	3 h	0 ↓*	1,2 ↓*	42,0 ↑*	48,1	8,6
Histaminergic nucleus E2	control	41,2	54,4	4,4	0	0
	30 min	29,4	51,4	19,2 ↑*	0	0
	3 h	0 ↓*	0	61,8 ↑*	37,4 ↑*	0,8
Mesencephalon						
Nucleus raphe magnus	control	54,3	43,8	1,9	0	0
	30 min	14,4 ↓*	83,3 ↑*	2,3	0	0
	3 h	7,8 ↓*	14,6 ↓*	64,1 ↑*	12,6 ↑*	1
Ventral tegmental area	control	46,2	6,6	28,5	13,2	5,5
	30 min	3 ↓*	4	39,4	47,5 ↑*	6,1
	3 h	0,7 ↓*	2,9	58,7 ↑*	29 ↑*	8,7
Substantia nigra, pars compacta	control	61,2	23,3	10,7	1,9	2,9
	30 min	17,7 ↓*	32,6	30,4	16,3	3
	3 h	7,5 ↓*	12,7	65,9 ↑*	10,4 ↑*	3,5
Substantia nigra, pars reticulata	control	59,5	28,6	11,9	0	0
	30 min	41,4	9,8 ↓*	29,3	17,1	2,4
	3 h	0 ↓*	29,8	45,6 ↑*	15,8 ↑*	8,8
Interpeduncular nucleus	control	74,4	4,4	12,3	6,1	2,7
	30 min	63,8	11,5	6,5	10,0	8,2
	3 h	1,8 ↓*	4,6	49,5	14,7	29,4 ↑*
Pons and medulla oblongata						
Adrenalinergic nucleus C1	control	31,2	56,9	10,1	1,8	0
	30 min	30,3	11,4 ↓*	44,3	8,9	5,1
	3 h	5,4 ↓*	24,3 ↓*	45,9	24,3	0
Trigeminal mesencephalic nucleus	control	45,7	34,4	17,1	2,9	0
	30 min	4 ↓*	34	48	12	2
	3 h	2,2 ↓*	48,9	24,4	20	4,4
Hypoglossal nucleus	control	11,1	63	18,5	7,4	0
	30 min	78,8 ↑*	18,4	3,1	0	0
	3 h	1,9	5,7 ↓*	63,8 ↑*	26,7 ↑*	1,9
Nucleus prepositus hypoglossi	control	56,8	39,2	0	4	0
	30 min	19,8	67,6	12,6	0	0
	3 h	0 ↓*	3,5	20,1 ↑*	59,6 ↑*	16,9 ↑*
Spinal trigeminal nucleus	control	85,5	11,6	2,9	0	0
	30 min	53,3 ↓*	42,6 ↑*	4,1	0	0
	3 h	12,0 ↓*	20,5	33,7 ↑*	30,1 ↑*	3,6
Dorsal motor nucleus of vagus	control	32,3	60	7,7	0	0
	30 min	23,6 ↓*	34,6	38,2 ↑*	3,6	0
	3 h	0 ↓*	4,3 ↓*	65,7	30 ↑*	0
Medullary reticular nucleus (ventral part)	control	61	34,5	4,5	0	0

Medullary reticular nucleus (ventral part)	30 min	42,5	45,3 ↑*	11,3	0,9	0
	3 h	1,5 ↓*	5,3 ↓*	64,9 ↑*	26,7 ↑*	1,5
Medullary reticular nucleus (dorsal part)	control	69,4	23,4	7,2	0	0
	30 min	46,6	47,9 ↑**	5,5	0	0
	3 h	1 ↓*	3,1 ↓*	62,9 ↑*	32 ↑*	1
Facial nucleus	control	50,9	35,5	11,5	2,1	0
	30 min	51,1	35,6	9,5	3,5	0,3
	3 h	14,8 ↓*	19,4	49,1 ↑*	13,0	3,7
Gigantocellular nucleus	control	58,9	33,5	7,2	0,4	0
	30 min	14,7 ↓*	69 ↑*	13,6 ↑*	1,9	0,8
	3 h	6,4 ↓**	15,4 ↓**	62,8 ↑*	11,5 ↑*	3,8
Gracile nucleus	control	68,3	29,3	2,4	0	0
	30 min	17 ↓*	75,4 ↑*	5,9 ↑*	1,1	0,6
	3 h	0 ↓*	19,4	57 ↑*	23,4 ↑*	0,2
Cuneate nucleus	control	44,4	40,1	15,5	0	0
	30 min	16,8 ↓*	52 ↑*	25,2 ↑*	3,2 ↑*	0
	3 h	0 ↓*	24,8	48,1 ↑*	26,6 ↑*	0,5
Medial vestibular nucleus	control	33,5	53,1	11,8	1	0,6
	30 min	8,5 ↓*	82 ↑*	8,4	0,9	0,2
	3 h	5,6 ↓*	4,7 ↓*	43,0	41,1 ↑*	5,6
Cerebellum						
Paraflocculus, Purkinje cells	control	42,9	53,6	3,6	0	0
	30 min	9,3	30,2	34,9	11,6	14 ↑*
	3 h	0 ↓*	13,3	52 ↑*	14,7 ↑*	20 ↑*
Simple lobule, Purkinje cells	control	72,7	15,9	9,1	2,3	0
	30 min	18,9	35,9	17,0	15,1	13,2
	3 h	0 ↓*	1,2	21	42 ↑*	25,8 ↑*
Paramedian lobule, Purkinje cells	control	75	18,8	6,3	0	0
	30 min	0 ↓*	39,5	47,4 ↑*	10,5	2,6
	3 h	4,2 ↓*	16,7	50,0 ↑*	25,0 ↑*	4,2
Pyramidal, Purkinje cells	control	68,8	22,9	4,2	4,2	0
	30 min	3,4 ↓*	50,9	28,8	11,9	5,1
	3 h	0 ↓*	1,6	34,9 ↑*	30,2 ↑*	33,3 ↑*
Interposed nucleus	control	35,8	41,5	17	5,7	0
	30 min	4,8 ↓*	47,6	38,1	9,5	0
	3 h	7,5	20 ↓*	17,5	50 ↑*	5
Medial nucleus	control	56,9	13,6	15,9	13,6	0
	30 min	3,6 ↓*	45,5	29,1	14,6	7,2
	3 h	2,4 ↓*	24,4	34,1	26,8	12,2
Lateral nucleus	control	15,5	48,3	32,8	1,7	1,7
	30 min	14	18,6	51,2	9,3	6,9
	3 h	12,2	14,3 ↓*	34,7	28,6 ↑*	10,2

The most significant changes in neuronal chromatophilia in SCI are found in the telencephalon and diencephalon. Among the studied structures of the telencephalon, neocortical regions are

the most sensitive to SCI. The reaction of the allocortex structures is diverse, with the piriform cortex being the most stable and the mitral cells of the olfactory bulbs being the least stable. The

sensitivity of neurons varies in different fields of the hippocampus. In the hippocampal CA3 and dentate gyrus fields neurons showed the least pronounced changes (Figure 1). Within the diencephalon the sensitivity in ischemia is not the same. The neurons of the midbrain, pons, and medulla oblongata are the most resistant to ligation of both common carotid arteries (Table 1). Relative stability is demonstrated by the nuclei of the cerebellum, but not by Purkinje cells (Table 1). Changes in ATP synthase and Ngb content in neurons of different parts of the rat brain during ischemia. After ischemia caused by ligation of the common carotid arteries the greatest

changes in ATP synthase immunoreactivity at the regional level were found in neurons of the neocortex and periallocortex of the telencephalon (Table 2). A significant decrease in immunoreactivity is observed in all the studied layers of the cortex after a 30-minute SCI (Table 2). After a 3-hour SCI, immunoreactivity is partially restored in comparison with the previous period or remains at the same low level (Table 2, Figure 2). An exception is the mitral cells of the olfactory bulb, in which after a 30-minute SCI a sharp increase in ATP synthase immunoreactivity is observed, but already after a 3-hour SCI it decreases to the initial level.

Table 2: Immunoreactivity of ATP synthase and Ngb in neurons with SCI: optical density units ×103 (*statistically significant difference compared to the control group, **difference compared to the previous term, p<0.05).

Structure, marker	Contents of ATP synthase and Ngb (Me (LQ; UQ))		
	control group	30 min SCI	3 h SCI
Telencephalon			
Mitral cells of the olfactory bulb	ATP-synthase	188,4 (146,9; 212,7)	284,1 (252,6; 309,5)*
	Ngb	156,7 (138,9; 174,3)	181,0 (170,1; 196,3)*
Piriform cortex, layer II	ATP-synthase	306,2 (241,6; 384,3)	243,1 (214,9; 270,5)*
	Ngb	185,2 (172,0; 197,0)	151,2 (140,3; 166,9)*
Hippocampus CA1, layer II	ATP-synthase	275,0 (229,7; 316,3)	248,8 (208,4; 280,7)*
	Ngb	209,2 (190,4; 226,9)	164,8 (154,8; 196,1)*
Hippocampus CA2, layer II	ATP-synthase	298,2 (265,3; 339,0)	321,1 (270,8; 382,0)
	Ngb	231,3 (217,9; 247,3)	204,8 (174,7; 221,1)*
Hippocampus CA3, layer II	ATP-synthase	294,5 (270,6; 341,2)	246,8 (207,6; 283,9)*
	Ngb	219,7 (193,2; 243,0)	177,5 (166,1; 198,2)*
Dentate gyrus, layer II	ATP-synthase	284,9 (250,8; 340,3)	230,1 (187,7; 307,2)*
	Ngb	186,6 (167,1; 213,8)	163,9 (149,8; 176,0)*
Retrosplenial agranular cortex, layer III	ATP-synthase	290,8 (261,7; 327,8)	191,6 (159,2; 242,9)*
	Ngb	226,3 (210,9; 244,2)	285,8 (251,8; 323,2)*
layer V	ATP-synthase	269,7 (250,1; 314,7)	182,7 (141,8; 224,8)*
	Ngb	240,4 (198,8; 259,2)	222,3 (197,9; 243,0)
layer VI	ATP-synthase	287,4 (250,1; 308,0)	149,7 (131,1; 258,4)*
	Ngb	244,6 (232,2; 260,7)	240,2 (219,2; 255,1)
Temporal cortex, layer III	ATP-synthase	294,6 (249,7; 313,7)	165,7 (89,9; 190,0)*
	Ngb	164,7 (153,1; 180,5)	165,5 (134,3; 206,8)
layer V	ATP-synthase	314,6 (275,0; 335,4)	194,8 (126,7; 245,0)*
	Ngb	179,4 (156,1; 191,3)	182,0 (150,4; 207,9)
layer VI	ATP-synthase	283,7 (246,1; 344,3)	198,7 (164,7; 261,5)*
	Ngb	167,6 (151,3; 185,2)	174,7 (156,2; 200,2)
Diencephalon			
Posterior thalamic group	ATP-synthase	255,9 (218,2; 303,0)	221,3 (190,9; 234,5)*
	Ngb	229,9 (204,7; 243,3)	174,1 (160,7; 201,6)*
Medial mammillary nucleus	ATP-synthase	333,4 (314,7; 360,9)	347,0 (292,4; 387,8)
	Ngb	217,6 (196,2; 232,3)	204,8 (190,9; 224,8)
Medial habenula of the thalamus	ATP-synthase	342,8 (283,0; 381,8)	256,0 (192,4; 289,7)*
			207,0 (170,0; 232,5)*, **

Medial habenula of the thalamus	Ngb	250,2 (226,7; 266,8)	168,6 (152,6; 180,3)*	144,1 (130,0; 157,5)*, **
Histaminergic nucleus E2	ATP-synthase	360,7 (315,8; 425,1)	327,0 (276,2; 370,0)*	252,7 (218,2; 294,1)*, **
	Ngb	305,0 (277,7; 317,0)	235,7 (218,2; 247,6)*	199,5 (176,3; 217,0)*, **
Pons and medulla oblongata				
Ventral tegmental area	ATP-synthase	271,3 (236,6; 292,4)	255,7 (206,8; 318,0)	267,3 (239,0; 302,8)
	Ngb	211,7 (188,5; 235,4)	237,6 (188,0; 269,4)	211,1 (194,9; 235,9)
Substantia nigra, pars compacta	ATP-synthase	327,0 (298,2; 349,2)	251,1 (208,1; 304,4)*	293,4 (270,3; 337,5)*, **
	Ngb	230,4 (210,0; 246,3)	170,9 (151,2; 184,3)*	141,4 (133,9; 151,3)*, **
Spinal trigeminal nucleus	ATP-synthase	332,4 (282,3; 365,1)	303,8 (270,9; 345,2)	310,3 (277,6; 377,9)
	Ngb	202,3 (177,2; 216,7)	190,7 (164,4; 227,8)	189,9 (170,2; 208,7)
Gigantocellular nucleus	ATP-synthase	340,5 (305,2; 381,0)	366,6 (327,5; 431,5)*	309,2 (288,8; 350,3)**
	Ngb	237,0 (215,5; 264,7)	183,9 (170,3; 194,1)*	191,6 (180,8; 208,7)*
Cerebellum				
Simple lobule, Purkinje cells	ATP-synthase	231,7 (219,1; 243,4)	247,0 (216,4; 279,4)	248,0 (234,6; 263,5)*
	Ngb	159,7 (147,6; 168,2)	155,3 (122,4; 169,4)	157,3 (146,7; 189,6)
Paraflocculus, Purkinje cells	ATP-synthase	270,3 (246,7; 296,9)	280,8 (259,6; 317,0)	220,0 (184,5; 245,9)*, **
	Ngb	171,0 (144,8; 183,7)	163,5 (135,6; 156,5)*	160,2 (134,3; 165,8)
Lateral nucleus	ATP-synthase	325,8 (284,6; 395,9)	308,1 (279,2; 345,9)	249,7 (198,3; 298,4)*, **
	Ngb	247,4 (190,3; 272,5)	214,0 (201,9; 224,1)	189,0 (174,5; 202,2)*, **
Interposed nucleus	ATP-synthase	348,6 (305,5; 400,2)	324,7 (298,4; 341,7)*	273,3 (230,8; 329,7)*, **
	Ngb	292,0 (268,3; 300,6)	224,3 (186,0; 241,4)*	226,0 (205,2; 237,8)*

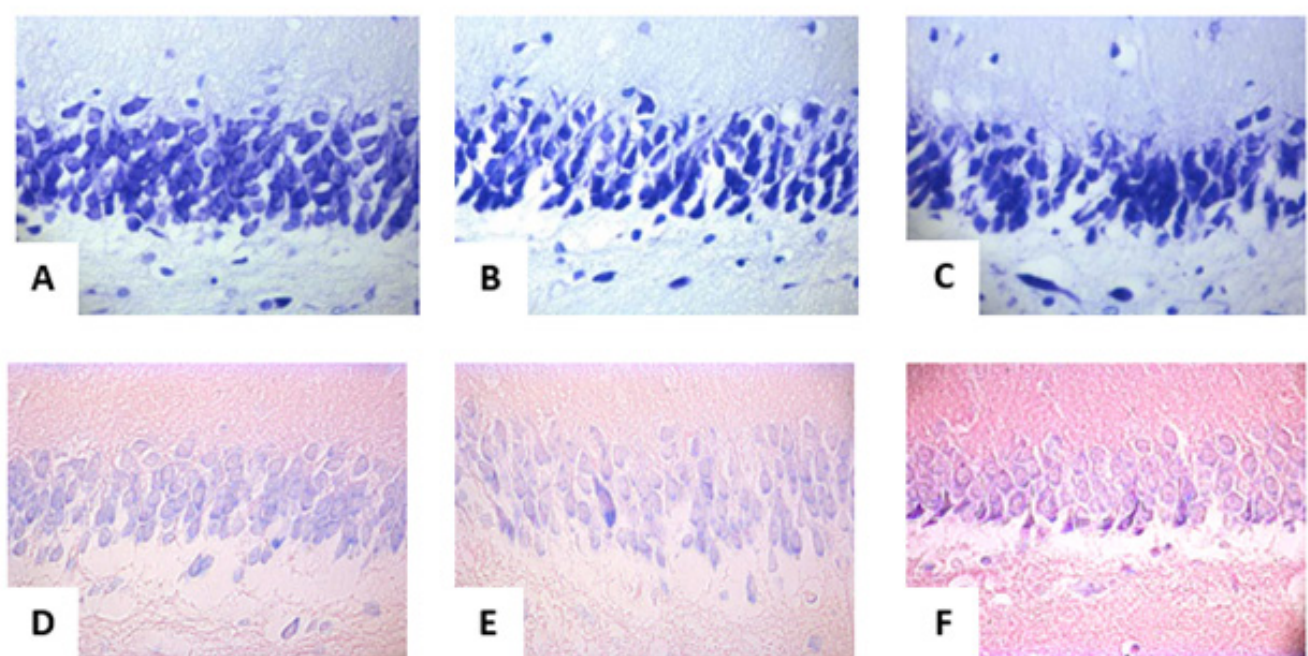


Figure 1: Dentate gyrus layer II neurons. A-C – Nissl staining, D-F – Viktorov staining. $\times 400$.

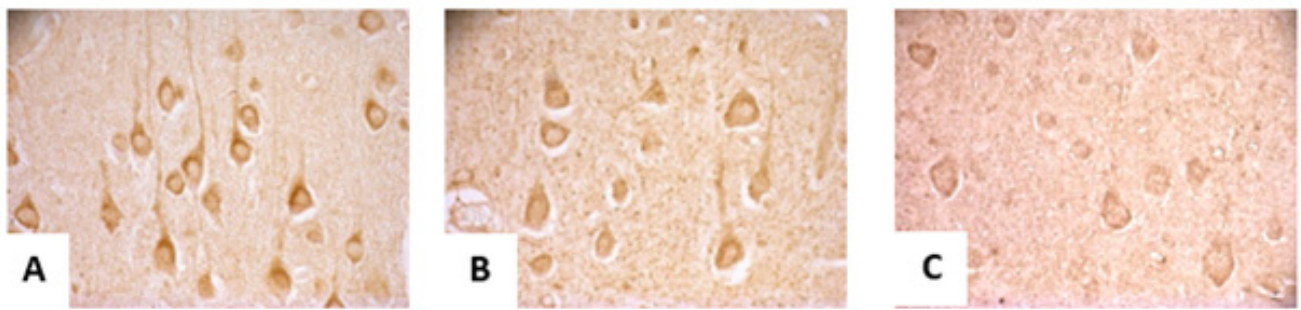


Figure 2: Temporal cortex layer V neurons. A – control group, B – 30-minute ischemia, C – 3-hour ischemia. Immunohistochemical staining of ATP-synthase. $\times 400$.

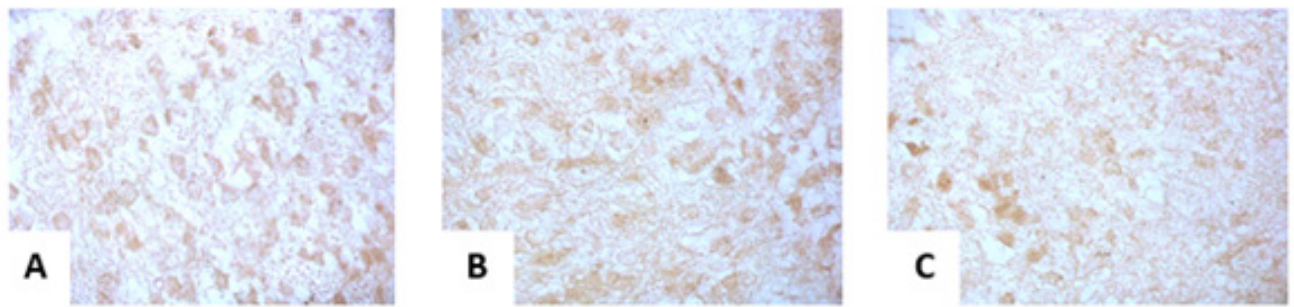


Figure 3: Medial habenula of the thalamus neurons. A – control group, B – 30-minute SCI, C – 3-hour SCI. Immunohistochemical staining of neuroglobin. $\times 400$.

Changes in ATP synthase immunoreactivity observed in the nuclei of the diencephalon are similar to those in the telencephalon. The nature of changes in immunoreactivity in neurons of the mesencephalon and medulla oblongata is less pronounced in comparison with the telencephalon and diencephalon (Table 2). In neurons of the nuclei of the cerebellum and Purkinje cells of the cerebellar cortex there are almost no changes in the immunoreactivity of ATP synthase after a 30-minute SCI, but already after a 3-hour SCI immunoreactivity in neurons noticeably decreases compared with control (Table 2).

Changes in Ngb immunoreactivity after SCI were found in neurons of all parts of the rat brain. A decrease in immunoreactivity (IR) is predominantly noted. However, its degree and speed differ (Table 2). The ancient piriform cortex is characterized by a rapid decrease after a 30-minute ischemia and an increase in immunoreactivity after a 3-hour exposure relative to a 30-minute SCI (Table 2). In the mitral cells of the olfactory bulb, on the contrary, Ngb-IR increases after a 30-minute SCI (Table 2). In the hippocampus and dentate gyrus, a decrease in IR Ngb is noted

in both terms (Table 2). In the layers of the periallocortex and neocortex, there is no decrease in IR after a 30-minute SCI, but there is a decrease after 3 hours (Table 2). In the neurons of the thalamic structures, Ngb-IR decreases already after a 30-minute ischemic exposure and continues after 3 hours (Table 2, Figure 3). Slower and less pronounced changes occur only in the medial mammillary nucleus (Table 2). In the midbrain and medulla oblongata, the changes are of a diverse nature - there is both a wave-like change in IR and its decrease already after a 30-minute exposure (Table 2). In one of the structures of the medulla oblongata, the spinal nucleus of the trigeminal nerve, no changes in Ngb-IR were found (Table 2). The structures of the cerebellum are characterized by different dynamics of changes in Ngb immunoreactivity. The least significant changes in Ngb-IR are observed in the Purkinje cells of the cerebellar cortex. The nuclei of the cerebellum are characterized by different times of Ngb-IR decrease (Table 2).

Relationships between the content of ATP synthase and Ngb and the degree of ischemic damage to brain neurons. The initial content of ATP synthase in neurons of all parts of the rat brain

positively correlates with the number of ischemic hyperchromic neurons ($r=0.43$; $p=0.04$) and negatively correlates with the number of shadow cells ($r=-0.43$; $p=0.04$) after 30 minutes of SCI. These correlations of ATP synthase in the brainstem and cerebellum with the number of postischemic hyperchromic shriveled up neurons ($r=0.62$; $p=0.03$) and shadow cells ($r=-0.69$; $p=0.01$) are more pronounced. At the same time, the initial content of ATP synthase in the telencephalon and diencephalon correlates more significantly with the number of hyperchromic shriveled neurons ($r=0.63$; $p=0.01$). In the telencephalon, the content of ATP synthase was negatively associated with the number of shadow cells after 30-minute ($r=-0.91$; $p=0.002$) and 3-hour SCI ($r=-0.74$; $p=0.04$). In addition, in the brainstem, including the diencephalon, normal amounts of ATP synthase are positively strongly correlated ($r=0.74$; $p=0.04$) with the number of hyperchromic neurons after a 30-minute SCI.

The negative relationship with shadow cells is especially obvious for Ngb, since most of the correlations found both in the entire brain and in its departments relate to this type of destructive changes in neurons. After a 30-minute SCI in all parts of the rat brain, a negative correlation is observed between the initial content of Ngb and the number of shadow cells after a 30-minute ischemia ($r=-0.505$, $p=0.01$). Similar in strength, but different in character, a positive correlation was found between the initial content of Ngb and the number of shadow cells after a 3-hour SCI ($r=0.45$; $p=0.027$). In the telencephalon and diencephalon, these correlations are somewhat higher: after 30 minutes ($r=-0.53$, $p=0.04$) and 3 hours of SCI ($r=-0.54$, $p=0.04$). In the brainstem and cerebellum, the correlation with the number of shadow cells after a 30-minute SCI is even higher ($r=-0.66$, $p=0.02$). In the brain stem after 3-hour SCI the correlation with Ngb amounts is strong and positive ($r=0.71$; $p=0.047$).

Discussion

The differences found confirm the literature data on a similar nature, but different severity of postischemic histological changes in neurons in different parts of the rat brain. According to our data, neurons of the telencephalon and diencephalon are damaged faster and more severely after ligation of the common carotid arteries. The sensitivity of neurons within the telencephalon is also heterogeneous as previously reported by other authors on the example of different sensitivity of the fields of the hippocampus and dentate gyrus to ischemia, detected using light, electron microscopy, and biochemical methods [3-6]. Since the telencephalon and diencephalon have minimal regional differences in blood supply, it is objective to compare the sensitivity of their structures. Compared with the telencephalon, no structures of the diencephalon can be called stable based on changes in the number of neurons with

different types of cytoplasmic chromatophilia. Also a comparison of changes in the structures of the diencephalon and the structures of the telencephalon most sensitive to subtotal ischemia (especially in neocortex) confirms the data on the relative lower sensitivity of populations of diencephalon neurons to ischemia [7]. In the cerebellum, the Purkinje cells of the cortex are more sensitive to subtotal cerebral ischemia. The high sensitivity of Purkinje cells to ischemia *in vivo* and *in vitro* was also reported by previous authors [5,8].

The obtained data on changes in the content of ATP synthase in neurons of different parts of the rat brain after ligation of the common carotid arteries demonstrate a different degree and rate of decrease in the content of ATP synthase, which may be due to different blood supply to the studied parts of the brain, as well as different sensitivity of individual populations of rat brain neurons in departments, possibly due to their different function, metabolic status, and neurotransmitter nature. The most significant and rapid decrease in the content of ATP synthase is a characteristic of the structures of the telencephalon of the rat which account for the greatest degree of ischemic impact in this experimental model. However, the rate and degree of decrease in the content of ATP synthase vary. Differences in the sensitivity of neurons in the parietal cortex and hippocampus to ischemia were previously reported [9,10]. The nature of changes in the content of ATP synthase in the neurons of the structures of the diencephalon vary too. The selective sensitivity of thalamic and hypothalamic neurons to ischemia has been described in the literature [7,11,12], but changes in the ATP synthase of these neurons have not been described. Despite the fact that the thalamus is intensively supplied with blood due to high metabolic demands and has a well-developed network of collaterals, the nature of changes in its structures is very different. In the posterior group of nuclei of the thalamus after prolonged ischemic exposure the level of ATP synthase immunoreactivity is restored, while in neurons of the medial habenular nucleus, immunoreactivity decreases throughout all periods of exposure. For histaminergic neurons of the hypothalamus (E2 nucleus), tolerance of ATP synthase to ischemic effects was not revealed.

From the literature data it is known that in the neurons of this nucleus after 30-minute ischemia, not only changes indicating the activation of synthetic processes predominate but signs of destruction of ultrastructure's are already observed [13], which may well correspond to a 9% decrease in ATP synthase after 30 min SCI. The obtained data on changes in the immunoreactivity of ATP synthase in neurons of the midbrain and medulla oblongata indicate a lower susceptibility of their neurons to changes in the content of ATP synthase during ligation of the common carotid arteries. Perhaps this is due to the preservation of collateral blood supply due to the preserved spinal arteries. However, a

structure was noted - substantia nigra - for which a sharp decrease in the content of ATP synthase was found after a 30-minute SCI. This pattern of changes is probably due to a large proportion of ischemia-sensitive dopaminergic neurons forming that structure [14] and a lower mitochondrial mass in these neurons compared to other midbrain structures (in particular, in comparison with the upper tegmental region) [15]. However, after a 3-hour SCI, the content of ATP synthase in them partially normalizes, possibly due to collateral circulation from the vertebral and basilar arteries. In the neurons of the cerebellar structures, the immunoreactivity of ATP synthase does not change during 30-minute subtotal ischemia but changes appear after 3-hour SCI.

The changes found allow us to speak about the different stability of the oxygen depot in the structures depending on the phylogenetic age: younger periallocortex, neocortex, and cerebellar cortex can be distinguished as structures with a more stable oxygen depot, since a 30-minute subtotal ischemia does not lead to a decrease in the Ngb content in them, while the oxygen depot in the allocortex, brain stem and cerebellar nuclei rapidly decreases. The lower sensitivity of the oxygen depot of phylogenetically young structures during ischemia was previously noted in the literature [16], but the factors that determine this difference have not yet been identified. The reason may be earlier activation of the neuroprotective function of neuroglobin in hippocampal neurons, due to a significantly higher level of neuronal nitric oxide synthase (nNOS) during oxygen-glucose deprivation, compared with cortical neurons [17]. The instability of the oxygen depot depends on the duration of the ischemic effect. After a 3-hour ischemia, the content of Ngb in the neurons of most structures decreases more significantly than after a 30-minute ischemia. It is important to note the rare cases of an increase in Ngb relative to the control level after a 3-hour subtotal cerebral ischemia, which is consistent with the data of other studies on an increase in Ngb in nerve cells with normal expression of this protein [18].

According to the nature of changes in cytoplasmic chromatophilia and ischemic degeneration of neurons and, accordingly, the features of changes in the content of ATP synthase and Ngb in them during ischemia, several main groups of neurons can be distinguished. First of all, these are neurons with minor and reversible ischemic destructive damage. These include only neurons of layer II of the piriform cortex, which combine a gradual decrease in the amount of ATP synthase with the preservation of the Ngb level. With a gradual decrease in the content of ATP synthase, as well as a gradual decrease in the amount of Ngb during a 3-hour ischemic effect, more significant changes are noted than in the previous group, but these changes are still reversible - an increase in the proportions of hypochromic and hyperchromic neurons. These structures include the lateral and intermediate nuclei of the cerebellum. With a later

onset of a decrease in the level of ATP synthase and a rapid decrease in the amount of Ngb (already after a 30-minute subtotal ischemia), an increase in the proportion of shadow cells is noted, and after a 3-hour ischemia, an increase in the proportions of hyperchromic shriveled up and hypochromic cells, the number also continues to increase in shadow cells. Such changes were noted in the Purkinje cells of the cerebellar cortex. While maintaining the amount of Ngb, and a late increase in the content of ATP synthase - as, for example, occurs in Purkinje cells of a simple lobule of the cerebellar cortex, there is an increase in the proportions of hypochromic neurons and shadow cells.

With an equal decrease of the amount of Ngb with a relatively late decrease in the content of ATP synthase (in neurons of layer II of the CA2 field of the hippocampus), hyperchromic shriveled neurons appear as the duration of exposure increases. While maintaining the levels of ATP synthase and Ngb as it happens in the ventral region of the tegmentum and the spinal nucleus of the trigeminal nerve, after a 30-minute ischemic exposure the first reversible changes appear and after a 3-hour exposure. A synchronous decrease in the amount of both proteins (in layer II CA3 of the hippocampal field, dentate gyrus, in the medial habenular nucleus of the thalamus, the histaminergic nucleus E2 and the gigantocellular nucleus) leads to early irreversible changes as early as 30 minutes after subtotal ischemia, and their aggravation after 3 hours of ischemia, including with the appearance of shadow cells. In the mitral cells of the olfactory bulb after a 30-minute subtotal ischemia, there is a sharp increase in the number of shriveled up, hypochromic neurons and shadow cells, which coincides with an increase in the content of ATP synthase in them and an increase in the amount of Ngb. However, after a 3-hour exposure, only an increased number of hyperchromic shriveled up neurons remains, which is accompanied by a decrease in ATP synthase in them and the preservation of an increased content of Ngb. In the other structures studied, which are characterized by very pronounced reversible and irreversible changes in cytoplasmic chromatophilia, a common feature is a decrease in the amount of Ngb with various changes in ATP synthase.

The results of the correlation analysis showed that a high initial content of ATP synthase is associated with a greater probability of neuronal shrinkage, but a lower probability of their transformation into shadow cells (especially for the telencephalon). Therefore, ATP synthase determines the path along which the ischemic destruction of neurons will proceed: its high initial level suggests shrinkage of neurons, and its low initial level implies transformation into shadow cells. Shrinkage of neurons in this case is explained by the accumulation of intracellular Na⁺ due to dysfunction of the energy-dependent Na⁺ pump during ischemia [19-21], which inevitably leads to irreversible damage to mitochondria [23,24] and can be

expressed in a change in the shape of perikaryons, chromatophilia of neuronal cytoplasm, opening of pathological mitochondrial pores and further lead to cell death [24]. The revealed negative correlations between the amount of Ngb and shadow cells demonstrate the protective effect of Ngb during short-term ischemic exposure, especially in the brainstem and cerebellum. Previously, information was cited in the literature that casts doubt on the neuroprotective role of Ngb at its endogenous amounts [25,26]. However, our data indicate that at a higher initial content of Ngb in neurons, their ischemic degeneration and transformation into shadow cells in the early period of SCI is lower, especially in the brainstem and cerebellum. This demonstrates for the first time the neuroprotective effect of Ngb on ischemia in non-mutated individuals [27,28].

Conclusion

The results of the study show that during subtotal cerebral ischemia in the neurons of the structures of different parts of the rat brain, there is a significant change in the ratio of neurons according to the type of cytoplasmic chromatophilia, which indicates the presence of both reversible and irreversible histological changes. The most vulnerable are the neurons of the telencephalon structures, especially the periallocortex and neocortex. The impact of unfavorable factors in subtotal cerebral ischemia has a different effect on the rate and degree of change in the amounts of ATP synthase in the cells of the structures of different departments. The most significant and rapid changes are typical for the structures of the telencephalon, while the least significant and slow are observed in the medulla oblongata and cerebellum. The nature of the dynamics of ATP synthase and Ngb potentially determines the path of neuronal destruction in cerebral subtotal ischemia. ATP synthase determines the path along which the ischemic destruction of neurons will proceed: its high initial level suggests shrinkage of neurons, and its low initial level implies transformation into shadow cells, which is especially pronounced in the case of the telencephalon. Preservation of the levels of ATP synthase and Ngb, as well as a decrease in the content of Ngb do not guarantee the protection of cells from transformation into pathological forms of neurons. Less serious changes in neuronal chromatophilia are noted when the Ngb content is preserved in combination with a decrease in the amount of ATP synthase. Negative outcome occurs with a decrease in the content of Ngb.

References

1. Paxinos, G (2007) The rat brain in stereotaxic coordinates. G Paxinos, C Watson, 6th (Edn.). London: Acad. Pres Pp: 448.
2. IV Victorov, K Prass, U Dirnagl (2000) Improved selective, simple, and contrast staining of acidophilic neurons with vanadium acid fuchsin. *Brain Res Protoc* 5(2): 135-139.
3. T Kirino, K Sano (1984) Selective vulnerability in the gerbil hippocampus following transient ischemia. *Acta neuropathological* 62 (3): 201-208.
4. T Kuroiwa, P Bonnekoh, KA Hossmann (1990) Prevention of postischemic hyperthermia prevents ischemic injury of CA1 neurons in gerbils. *Journal of Cerebral Blood Flow & Metabolism* 10: 550-556.
5. M Horn, W Schlotte (1992) Delayed neuronal death and delayed neuronal recovery in the human brain following global ischemia. *Acta Neuropathol* 85(1): 79-87.
6. I Ferrer, MA Soriano, A Vidal, AM Planas (1995) Survival of parvalbumin-immunoreactive neurons in the gerbil hippocampus following transient forebrain ischemia does not depend on HSP-70 protein induction. *Brain Research* 692: 41-46.
7. CD. Brisson, RD Andrew (2012) A neuronal population in hypothalamus that dramatically resists acute ischemic injury compared to neocortex. *Journal of Neurophysiology* 108(2): 419-430.
8. J Brasko, P Rai, MK Sabol, P Patrikios, DT Ross (1995) The AMPA antagonist NBQX provides partial protection of rat cerebellar Purkinje cells after cardiac arrest and resuscitation. *Brain Research* 699: 133-138.
9. LI Bon, N Ye Maksimovich, SM Zimatkin (2018) Histological changes in the parietal cortex and hippocampus of rats after incomplete cerebral ischemia. *Journal of Grodno State Medical University* 16 (4): 419-423.
10. LI Bon, N Ye Maksimovich, SM Zimatkin, NA Valko (2019) Morphological disturbances of the parietal cortex and hippocampus neurons in the dynamics of subtotal cerebral ischemia. *Orenburg medical herald* 2(26): 6-41.
11. T Inoue, H Kato, T Araki, K Kogure (1992) Emphasized selective vulnerability after repeated nonlethal cerebral ischemic insults in rats. *Stroke* 23 (5): 739-745.
12. RM Dijkhuizen, S Knollema, HB van der Worp, GJ Ter Horst, DJ De Wildt, et al. (1998) Dynamics of cerebral tissue injury and perfusion after temporary hypoxia-ischemia in the rat: evidence for region-specific sensitivity and delayed damage. *Stroke* 29(3): 695-704.
13. VB Kuzniatsova, Ye Krishtofik, VA Kazliakouskaya (2015) Ultrastructural features of neurons of histaminergic nucleus E2 in rat hypothalamus after subtotal thirty-minute cerebral ischemia and reperfusion. *Journal of Grodno State Medical University* 1: 44-48.
14. Chee Yean Chung, Hyemyung Seo, Kai Christian Sonntag, Andrew Brooks, Ling Lin, et al. (2005) Cell type-specific gene expression of midbrain dopaminergic neurons reveals molecules involved in their vulnerability and protection. *Hum Mol Genet* 14(13): 1709-1725.
15. Chang-Lin Liang, Tom T Wang, Kate Luby-Phelps, Dwight C German (2007) Mitochondria mass is low in mouse substantia nigra dopamine neurons: implications for Parkinson's disease. *Exp Neurol* 203 (2): 370-380.
16. Aijia Shang, Dingbiao Zhou, Lihong Wang, Yan Gao, Ming Fan, et al. (2006) Increased neuroglobin levels in the cerebral cortex and serum after ischemia-reperfusion insults. *Brain Res* 1078(1): 219-226.
17. Xiangning Jiang, Dezhi Mu, Catherine Manabat, Anita A Koshy, Stephan Christen, et al. (2004) Differential vulnerability of immature murine neurons to oxygen-glucose deprivation. *Exp Neurol* 190 (1): 224-232.
18. Rainald Schmidt-Kastner, Mark Haberkamp, Christoph Schmitz, Thomas Hankeln, Thorsten Burmester (2006) Neuroglobin mRNA expression after transient global brain ischemia and prolonged hypoxia in cell culture. *Brain Research* 1103(1): 173-180.
19. MM Pike, M Kitakaze, E Marban (1990) ²³Na-NMR measurements of intracellular sodium in intact perfused ferret hearts during ischemia and reperfusion. *Am J Physiol* 259(6 pt. 2): H1767-1773.

20. NB Butwell, R Ramasamy, I Lazar, AD Sherry, CR Malloy (1993) Effect of lidocaine on contracture, intracellular sodium, and pH in ischemic rat hearts. Am. J. Physiol 264(6 pt. 2): H1884-9.
21. MC Haigney, EG Lakatta, MD Stern, HS Silverman (1994) Sodium channel blockade reduces hypoxic sodium loading and sodium-dependent calcium loading. Circulation 90(1): 391-399.
22. Kenichi Imahashi, Hideo Kusuoka, Katsuji Hashimoto, Jun Yoshioka, Hitoshi Yamaguchi, et al. (1999) Intracellular sodium accumulation during ischemia as the substrate for reperfusion injury. Circ Res 84 (12): 1401-1406.
23. Takeshi Iwai, Kouichi Tanonaka, Rie Inoue, Sayaka Kasahara, Naoki Kamo, et al. (2002) Mitochondrial damage during ischemia determines post-ischemic contractile dysfunction in perfused rat heart. J Mol Cell Cardiol 34(7): 725-738.
24. Keisuke Kawasaki, Yoshiaki Suzuki, Hisao Yamamura, Yuji Imaizumi (2019) Rapid Na⁺ accumulation by a sustained action potential impairs mitochondria function and induces apoptosis in HEK293 cells expressing non-inactivating Na⁺ channels. Biochem Biophys Res Commun 513(1): 269-274.
25. Zindy Raida, Christian Ansgar Hundahl, Jesper Kelsen, Jens Randel Nyengaard, Anders Hay-Schmidt (2012) Reduced infarct size in neuroglobin-null mice after experimental stroke in vivo. Exp. Transl. Stroke. Med 4(1): e15.
26. Valentina Di Pietro, Giacomo Lazzarino, Angela Maria Amorini, Barbara Tavazzi, Serafina D'Urso, et al. (2014) Neuroglobin expression and oxidant/antioxidant balance after graded traumatic brain injury in the rat. Free Radic Biol Med 69: 258-264.
27. Directive 2010/63/EU of the European Parliament and Council of the European Union of 22 Sept 2010 on animal protection, used in the scientific purposes.
28. (2017) Korzhevskiy DE (Edn.). Immunohistochemical study of the brain. Saint-Petersburg: Spec Lit, Pp:143.

ISSN: 2574-1241

DOI: [10.26717/BJSTR.2022.46.007363](https://doi.org/10.26717/BJSTR.2022.46.007363)

LI Bon. Biomed J Sci & Tech Res



This work is licensed under Creative Commons Attribution 4.0 License

Submission Link: <https://biomedres.us/submit-manuscript.php>



Assets of Publishing with us

- Global archiving of articles
- Immediate, unrestricted online access
- Rigorous Peer Review Process
- Authors Retain Copyrights
- Unique DOI for all articles

<https://biomedres.us/>